



# Journal of Applied Sciences

ISSN 1812-5654

**science**  
alert

**ANSI***net*  
an open access publisher  
<http://ansinet.com>

## Prediction of Supersonic Flow over Compression Corner

Nor Azwadi Che Sidik and Koh Wei Loon

Department of Thermo Fluid, Faculty of Mechanical Engineering, Universiti Teknologi Malaysia,  
81310 UTM Skudai, Johor, Malaysia

**Abstract:** Numerical investigation of supersonic flow over two-dimensional compression corner. The laminar viscous and inviscid flow equations were discretised using finite different technique and the computer program code was developed using MATLAB. The analysis was conducted for corner angles of 5 to 20° and the flow velocity was varied from 2.5 to Mach 3.5. In the current study, we found that the magnitudes of peak pressure and recirculation region on the ramp were significantly affected by the flow velocity and corner angles. Results obtained were validated by using analytical solutions as well as from previous researchers and they are found to be in good agreement.

**Key words:** Finite difference, shock wave, compression corner, supersonic flow, FLUENT

### INTRODUCTION

The occurrence of supersonic/hypersonic flow over compression corner can be found on many practical high-speed flow applications, to name a few, the control surfaces (such as elevons, wing- and body-flaps) and air intake compression ramps of the air-breathing propulsion system on re-entry vehicles as well as high-speed aircrafts. The dramatic significance of such phenomenon in application have induced much attention from many researchers, hence lots of related studies, either experimentally or numerically, have been conducted extensively over the past few decades.

As the high-speed flow pass through the compression corner, it would first experience compressive disturbance and subsequently its streamline is deflected, accompanying by the formation of oblique shock wave. The development of shock wave can be elucidated as followed; the disturbance waves caused by the corner would try to propagate with sonic speed to surrounding regions, including directly upstream, for communicating the changes of energy and momentum to other regions of the flow. Nevertheless, since the incoming mainstream is supersonic/hypersonic, the disturbance waves could no longer travel upstream. Instead, they would coalesce a short distance ahead of the corner into a thin layer which is in fact the shock wave itself. This case is particularly true for inviscid flow, where the pressure of the flow increases discontinuously across the shock wave.

In reality, the viscosity of the flow exists and must also be taken into account; thus boundary layer would

form on the surface due to the viscous nature of the flow (no-slip condition). In the presence of boundary layer, the pressure rise along the surface does not occur abruptly since the disturbance could travel upstream through the subsonic region near the wall; rendering the boundary layer to be subjected to a rapid yet continuous pressure change. For sufficiently strong shock, the interaction between shock wave and the boundary layer would lead to another interesting phenomenon, i.e., the separation and reattachment of flow as well as the formation of recirculation region around the corner. In this case, the boundary layer separates ahead of the corner and eventually reattaches downstream of the corner which gives rise to a recirculation bubble in the shape similar to a small-angled wedge. Hence, the compression process happens in two stages; first through the separation region and then through the reattachment region, yielding separation shock and reattachment shock, respectively (Dogrusoz and Kavsoglu, 2001).

Holden and Moselle (1969) had conducted experimental research for both laminar and turbulent shock wave-boundary layer interactions from supersonic through hypersonic regime. The results established that the upstream influence rises with the ramp angle and decreases with Mach number and it is also affected by Reynolds number as well (weakly in fully turbulent mode). Further experimental studies demonstrated that the upstream influence and separation length (indicating the level of intensity of shockwave-boundary layer interaction) increases with the ramp angle (for fixed Mach and Reynolds numbers) and decreases with Mach number

(for fixed ramp angle and Reynolds numbers). Similarities are observed in the overall flow features for both laminar and turbulent conditions, the major differences being the interaction extent (i.e., characteristic scale) and the pressure and thermal loads (i.e., the strength).

Carter (1972) had conducted the numerical investigations for the supersonic laminar flow over a 2-dimensional compression corner. The steady-state solutions were obtained by marching the unsteady Navier-Stokes equations over time. He employed the finite-difference method proposed by Brailovskaya (1971) which is first-order accurate in time and second-order accurate in space. Besides, variable grid formulation by Cebeci *et al.* (1970), where the grid is expanded at a constant rate from the wall, was imposed. The experimental results by Kubota *et al.* (1968) were utilized to compare with the numerical solution and found to be in good agreement. On the other hand, Hung and MacCormack (1976) adopted an efficient time-splitting finite difference scheme which is second-order accurate in both time and space to obtain steady state solutions of Navier-Stokes equations for supersonic and hypersonic laminar flows over a compression corner. They obtained favourable comparisons with the previous calculations and experiments such as by Holden and Moselle (1969) which indicated the reliability of their results.

Numerical investigation of the similar problem had also been conducted by Dwoyer (1973) with the purpose of developing a reliable solution technique for the shock-boundary layer interaction problem applicable over a wide range of flow parameters. In this case, he utilized a finite-difference interacting boundary layer scheme. The boundary layer equations were coupled to the inviscid free stream by the tangent wedge relationships. To recover the profiles of reverse flow, the method is somewhat adapted following the work of Werle and Bertke (1972), in which the boundary condition on the continuity equation was applied at the outer edge and this value is cycled until the prescribed wall boundary value is met. In addition, Dogrusoz and Kavsoglu (2001) had simulated the 2-dimensional hypersonic compression corner by employing Reynolds-Averaged Thin Layer Navier-Stokes equations for shock capturing purpose. Their results reported that the maxima in the pressure and heat transfer distributions increase with the corner angle. Furthermore, the separation region would also become larger for increased corner angle. The computed pressure and Stanton number were compared with the experimental results from Malinson *et al.* (1992) and found to be in better agreement for attached flow regions while discrepancies were observed for locations covered with large separation zone. The computed shock wave angles

were also found to be very close to the results from oblique shock theory.

The complexity and design challenges owing to these phenomena demand a thorough understanding of controlling measure and the quantitative prediction. The experimental investigation of Shock Wave-Boundary Layer Interaction (SWBLI) around the compression corner would generally demand rather extensive preparation and sophisticated equipments or facilities in the laboratory due to the requirement of high-speed flow. In contrast, numerical investigation or Computational Fluid Dynamic (CFD) offers much ease and convenience in the sense that the numerical experiment can be carried out to attain insight of the behaviour of the problem. Hence, in the present work, the supersonic flow over the compression corner will be investigated numerically for both steady, inviscid flow and steady, laminar flow cases. The effect of changes of velocity (Mach number) as well as ramp angle on the flow field properties will also be simulated and examined. Validation would be made using analytical approach available whenever possible to conduct a sensible checking on the result. Comparison will also be made with the results from the previous studies for further validation of the data.

**Numerical modeling:** The general Euler equations will be adopted as the governing equations in algorithm development of the MATLAB code for inviscid case which are rewritten as follows:

$$\nabla \cdot (\rho \mathbf{v}) = 0 \quad (1)$$

$$\nabla \cdot (\rho \mathbf{u} \mathbf{v}) = -\frac{\partial p}{\partial x} \quad (2)$$

$$\nabla \cdot (\rho \mathbf{v} \mathbf{v}) = -\frac{\partial p}{\partial y} \quad (3)$$

$$\nabla \cdot \left( \rho \left( \mathbf{e} + \frac{\mathbf{v}^2}{2} \right) \mathbf{v} \right) = -\frac{\partial (u p)}{\partial x} - \frac{\partial (v p)}{\partial y} \quad (4)$$

The grid generation for the present case is shown in Fig. 1a. The physical plane adopts a Cartesian coordinate system. The surface including the compression corner forms the lower boundary in this physical plane. The inflow boundary is placed at  $x = 0$  and the outflow boundary is at  $x = L$ . A horizontal line is chosen at the upper boundary at  $y = H$ . For computation using finite-difference scheme, such plane has to be converted into uniform rectangular-grid of computational plane, as shown in Fig. 1b. The computational plane is defined by  $\xi$ - $\eta$  coordinate system.

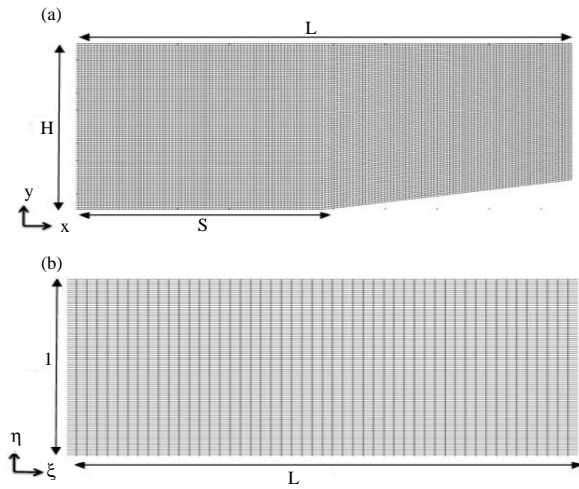


Fig. 1 (a-b): (a) Physical plane and (b) Computational planes for the numerical solution of the inviscid supersonic flow over compression corner problem

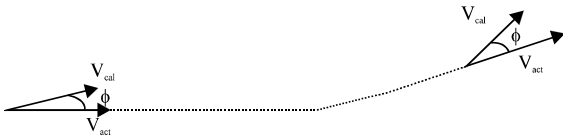


Fig. 2: Abbett's boundary conditions for a steady inviscid flow

Abbett's boundary condition (Anderson, 1995) is applied at the wall to ensure the inviscid flow to be tangent to the wall. The detailed procedures are illustrated in Fig. 2.

The calculated velocity make an angle  $\phi$  at the wall, where  $\phi = \tan^{-1}(v/\mu)$ . To correct the calculated velocity to ensure its tangency on the wall, assumes that the supersonic flow of  $v_{cal}$  is rotated through a local centered Prandtl-Meyer expansion wave so that the velocity vector is tangent to the wall. This yields a new velocity vector  $v_{act}$  which will be taken as the actual velocity tangent to the wall.

For the case of supersonic, viscous laminar flow over the compression corner, the governing equations can be written as follow:

$$\frac{\partial \rho}{\partial t} + \frac{\partial(\rho u)}{\partial x} + \frac{\partial(\rho v)}{\partial y} = 0 \quad (5)$$

$$\frac{\partial(\rho u)}{\partial t} + \frac{\partial(\rho u^2 + p)}{\partial x} + \frac{\partial(\rho uv)}{\partial y} = \frac{\partial \tau_{xx}}{\partial x} + \frac{\partial \tau_{xy}}{\partial y} \quad (6)$$

$$\frac{\partial(\rho v)}{\partial t} + \frac{\partial(\rho uv)}{\partial x} + \frac{\partial(\rho v^2 + p)}{\partial y} = \frac{\partial \tau_{yx}}{\partial x} + \frac{\partial \tau_{yy}}{\partial y} \quad (7)$$

$$\frac{\partial E}{\partial t} + \frac{\partial u(E + p)}{\partial x} + \frac{\partial v(E + p)}{\partial y} = \frac{\partial}{\partial x} \left( k \frac{\partial T}{\partial x} \right) + \frac{\partial}{\partial y} \left( k \frac{\partial T}{\partial y} \right) + \frac{\partial}{\partial x} (u \tau_{xx} + v \tau_{xy}) + \frac{\partial}{\partial y} (u \tau_{xy} + v \tau_{yy}) \quad (8)$$

where:

$$\tau_{xx} = 2\mu \frac{\partial u}{\partial x} - \frac{2}{3}\mu \left( \frac{\partial u}{\partial x} + \frac{\partial v}{\partial y} \right) \quad (9)$$

$$\tau_{xy} = \tau_{yx} = \mu \left( \frac{\partial u}{\partial x} + \frac{\partial v}{\partial y} \right) \quad (10)$$

$$\tau_{yy} = 2\mu \frac{\partial v}{\partial y} - \frac{2}{3}\mu \left( \frac{\partial u}{\partial x} + \frac{\partial v}{\partial y} \right) \quad (11)$$

$$E = \rho \left( e + \frac{u^2 + v^2}{2} \right) \quad (12)$$

Moreover, the air is assumed to be ideal gas and is viscous in nature. Therefore, ideal gas equation and Sutherlands semi-empirical equation are employed as well for the algorithm development:

$$p = \rho RT \quad (13)$$

and:

$$\frac{\mu}{\mu_r} = \left( \frac{T}{T_r} \right)^{\frac{3}{2}} \frac{T_r + S_0}{T + S_0} \quad (14)$$

Where:

$$\mu_r = 1.7894 \times 10^{-5}$$

$$T_r = 288K$$

$$S_0 = 110K$$

The type of grid for the viscous case is shown in Fig. 3. Notice that the grid is denser near the bottom of the wall in order to capture the flow field characteristic near the wall. The physical plane is then transformed into the computational plane of uniform rectangular grid which is suitable for the finite difference computation.

Since, the problem is a marching typed problem, the flow properties at each point must be set at  $t = 0$ . In this case, the properties at each grid point are initialized at free stream values, except for the points on the wall whereby

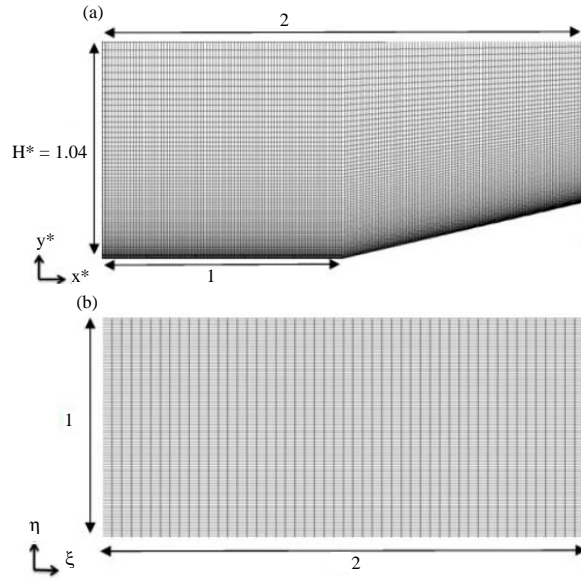


Fig. 3 (a-b): (a) Physical plan and (b) Computational planes for the numerical solution of the viscous laminar supersonic flow over compression corner problem

no-slip boundary condition and the wall temperature are imposed. Other boundary conditions are as shown in Fig. 4. The free stream condition is applied on the left of the domain to model the incoming supersonic flow. Wall conditions are applied at the lower boundary of the domain, whereby the no-slip condition would be imposed at this boundary due to the viscosity of the fluid. All other properties at the other boundaries are extrapolated from the interior points. The extrapolations from the interior are performed by using the two immediate neighbouring points.

In the present study, the equations are discretized using explicit MacCormack scheme with predictor-corrector step in the form of finite difference. Since the scheme used is of explicit formulation, the time step used has to satisfy the stability criterion. To determine the appropriate size of time step, the following version of Courant-Friedrichs-Lewy (CFL) criterion is adopted (Anderson, 1995):

$$\Delta t = \left[ \frac{|u_{i,j}|}{\Delta x} + \frac{|v_{i,j}|}{\Delta y} + a_{i,j} \sqrt{\frac{1}{\Delta x^2} + \frac{1}{\Delta y^2}} + 2v \left( \frac{1}{\Delta x^2} + \frac{1}{\Delta y^2} \right) \right]^{-1} \quad (15)$$

where:

$$v = \max \left[ \frac{\frac{4}{3} \mu (\gamma \mu / Pr)}{\rho_{i,j}} \right] \quad (16)$$

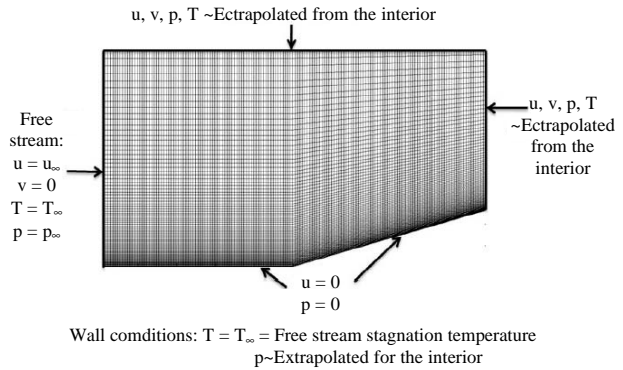


Fig. 4: Boundary conditions of the domain

$$\Delta t = \min [K \Delta t] \quad (17)$$

The solution is marched from initial condition until steady-state condition, where the deviation of the primitive variables from the previous time step is less than  $10^{-6}$ .

**Problem physics and numerical results:** In the previous section, we have discussed a numerical approach to predict supersonic flow over two-dimensional compression corner. This section will present the results obtained from the simulation of both inviscid and laminar cases. For the both cases, the pressure profiles will be plotted to investigate the effect of variable corner angles and free stream velocity (Mach number). Validation from other sources will also be provided.

Figure 5 shows the Mach number contour plot for the inviscid supersonic flow over the compression corner. Notice that there is oblique shock exists on the ramp and an abrupt change in flow velocity occurs across the shock. When the flow past over the compression corner, the flow streamline would be deflected upward, through the main bulk of the flow above the surface. This introduces compressive disturbance onto the flow. The disturbance signals would attempt to travel with sonic speed to the surrounding regions (upstream and downstream) to communicate the changes of momentum and energy to the nearby region. However, due to the supersonic flow of the free stream, this disturbance signals is unable to travel upstream. Rather, they would be carried downstream and form a thin layer at a short distance ahead of the corner which could be visualized as the shock wave.

Figure 6 shows the pressure profile for the inviscid flow of Mach 3 over the compression corner of variable angle. Note that an excellent agreement is found between the analytical results with the numerical results, except that there are some numerical oscillations exist on the curve near the corner which quickly diminish as progress

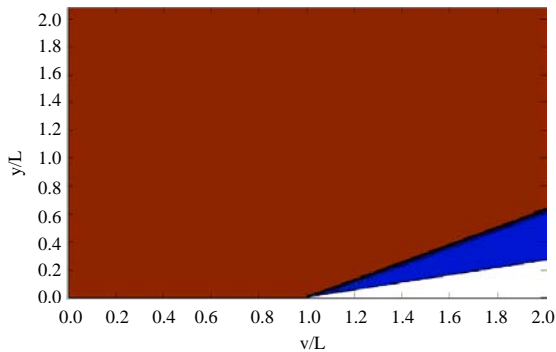


Fig. 5: Mach number contour plot for inviscid supersonic flow over compression corner of case 15 degree and free stream of Mach number 3

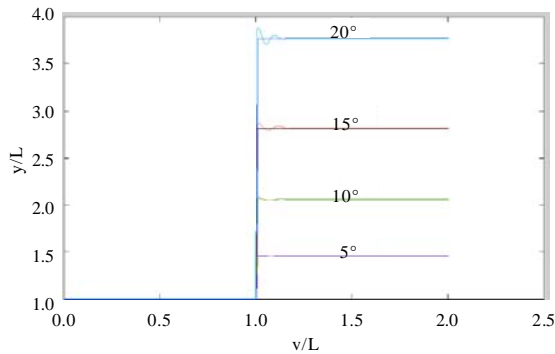


Fig. 6: Pressure profile for the inviscid flow of Mach 3 over the compression corner of variable angle

further from the corner. These oscillations would be due to the second-order nature of MacCormack scheme which tend to introduce oscillation around the discontinuity. Such discrepancies may be minimized by adopting other method such as upwind scheme to reduce the oscillation around the discontinuity. From Fig. 6, it can be observed that higher corner angle yields higher pressure as the flow passes through the compression corner. This may be elucidated by the fact that higher corner angle introduces larger compressive disturbance to the flow, hence there would be a larger momentum change as the flow passes over the corner which in turn induces larger pressure on the ramp.

In addition, the pressure profile for variable free stream velocity (Mach number) at corner angle 15 degree is presented as well on the Fig. 7. Again, the numerical result is found to agree very well with the analytical solution, despite of the numerical oscillation near the corner. It can be seen that higher free stream velocity would introduce larger pressure on the ramp. This is due

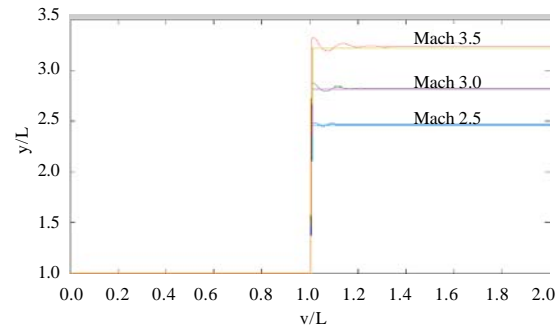


Fig. 7: Pressure profile for variable free stream velocity (Mach number) for inviscid case at corner angle 15 degree

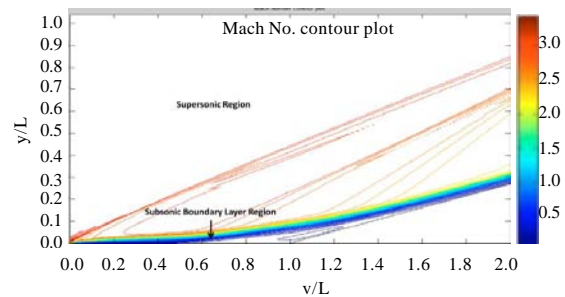


Fig. 8: General flowfield characteristic of the laminar supersonic flow over compression corner

to the higher momentum possessed by the flow of higher velocity and hence greater impact and pressure on the ramp as it flows over the corner.

Next, the flowfield characteristic of the laminar supersonic flow over compression corner will be investigated. From Fig. 8, notice that there exist both regions of supersonic and subsonic boundary layer in the domain, as opposed to the case of inviscid supersonic flow discussed previously. Such situation arises due to the fact that the air itself is viscous in nature which will tend to stick on the wall (no slip condition) as it passes through the flat plate and the ramp. As a result, boundary layer is thus formed on the wall. A closer view focus on the region around the corner is now taken, as shown in the Fig. 9. The leading edge shock arises due to the fact that the viscous flow from the farfield detects the flat plate as an obstacle and compressive disturbance would thus be generated, forming the leading edge shock. Notice that separation of flow occurs at the upstream boundary layer of the corner. Such phenomenon occurs due to the lack of sufficient momentum adverse pressure gradient induced by the corner. This results in the formation of recirculation region and this causes the boundary layer to thicken as



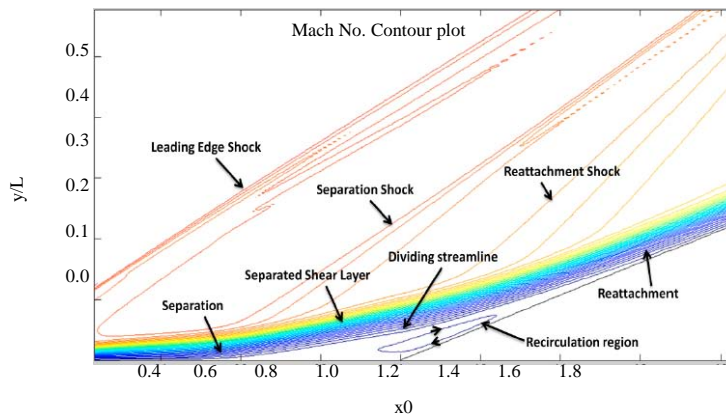


Fig. 9: Closer view on the region around corner

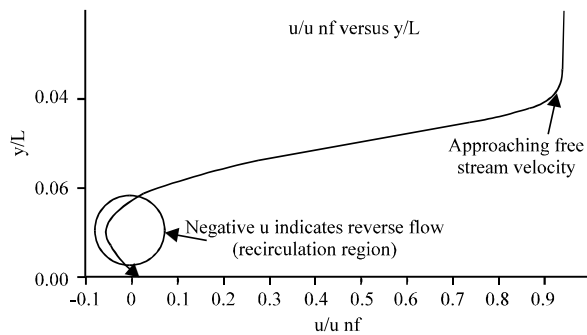


Fig. 10: Velocity profile across the recirculation region

well. Along the shear layer, the flow is accelerated by the action of viscous forces until it regains sufficient momentum to overcome the second pressure increase at the reattachment downstream. Overall, the flow experience two main compression stages, i.e., at the separation and reattachment regions which hence induces the separation shock as well as reattachment shock.

To gain closer look on the recirculation region, a section at the corner is taken to observe its velocity profile across the recirculation region, as shown in Fig. 10. From the velocity profile, it can be seen that there is a negative component of velocity which clearly indicates the reverse flow portion of the recirculation region. Notice also that further across the boundary layer, the velocity profile is approaching the free stream velocity which is similar to the case of typical boundary layer. The general trend of the pressure profile for the laminar supersonic flow over the compression corner is now investigated.

Figure 11 shows the pressure profile for the case of 15 degree corner angle with free stream of Mach 3. For the inviscid case, there is a sharp rise of pressure over the corner. On the other hand, the pressure profile for laminar case increases in a progressive manner. This can be

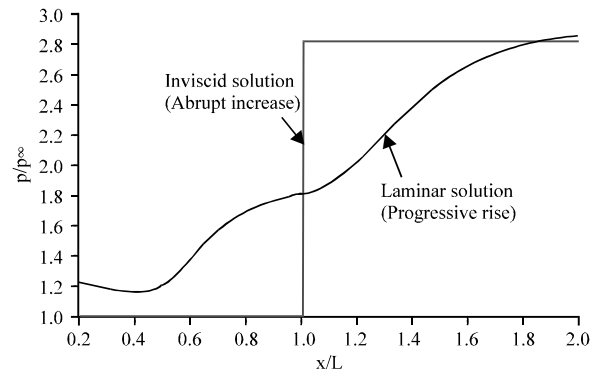


Fig. 11: Pressure profile for the case of 15 degree corner angle with free stream of Mach 3

explained by the existence of subsonic boundary layer near the wall which allows the compressive disturbance signal (pressure change) to be propagated and felt by both the upstream and downstream region of the corner, hence the pressure would increase in a more gradual manner as opposed to the abrupt increase for inviscid case.

There are also several other characteristics of the pressure profile worth to be noted. From Fig. 12, the existence of recirculation is denoted by the pressure plateau in the profile, where the pressure remains relatively constant for this region. On the other hand, the separation and reattachment point are indicated by the inflection points. Notice that the peak pressure shoots higher than that of the inviscid case. This phenomenon may be elucidated as follows. The recirculation region near the corner is separated from the main flow over the compression corner, thus it somehow acts as a wedge at the corner. Therefore, the flow would experience two stages of compression, i.e., immediately before the wedge (separation point) and right after the wedge (reattachment point). The pressure on the wedge (free shear layer on top

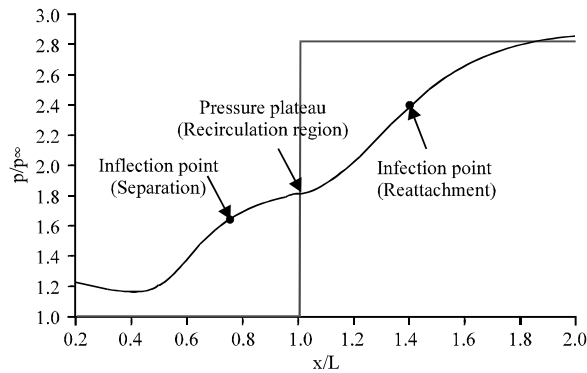


Fig. 12: Pressure profile for the case of 15 degree corner angle with free stream of Mach 3, with the indication of pressure plateau, as well as separation and reattachment point

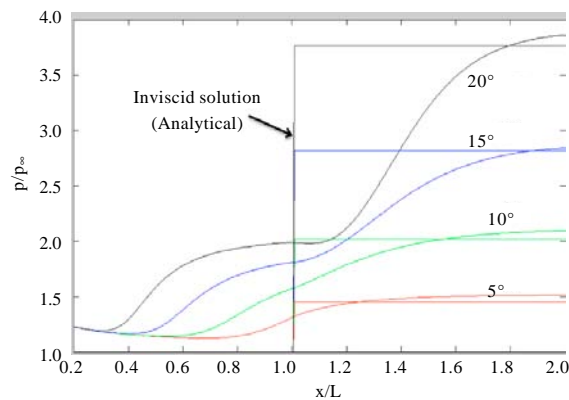
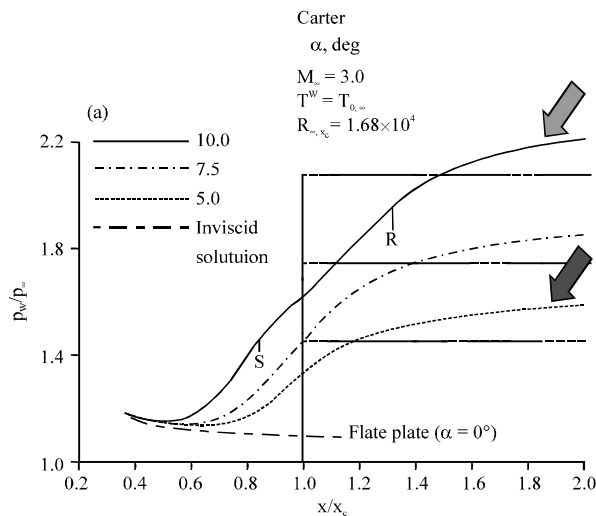


Fig. 13: Pressure profile for variable angle



of the recirculation) is relatively constant which is somehow similar to the case on the flat plate. Due to the two compression stages, hence it is not surprising that the peak pressure for the laminar case would shoot higher than that of the inviscid case.

Next, the effect of corner angle on pressure profile for laminar case at free stream of Mach 3 is investigated, as shown in Fig. 13. Four cases were selected for the analysis which are 5, 10 15 and 20 degree. From the graph, it can be seen that as the angle increases, the peak pressure increases as well. The larger compressive disturbance introduced by larger corner angle would account for this trend. Notice that the pressure plateau becomes flatter for larger corner angle. This signifies that the recirculation region is getting more pronounced.

In addition, the results from MATLAB had also been compared qualitatively with the one obtained from Carter (1972) for the case 5 degree and 10 degree, as shown in Fig. 14. Again, the Matlab results agree with the results from Carters very well, thus indicates the validity of the program.

Next, the effect of free stream velocity on the pressure profile at corner angle 15 degree is discussed. Three cases were selected, i.e., 2.5, 3 and Mach 3.5, as shown in Fig. 15. Note that the peak pressure increases with the Mach number of the free stream. This is because higher flow velocity possesses larger momentum, thus greater impact would be induced as it flows over the corner which therefore leads to higher peak pressure.

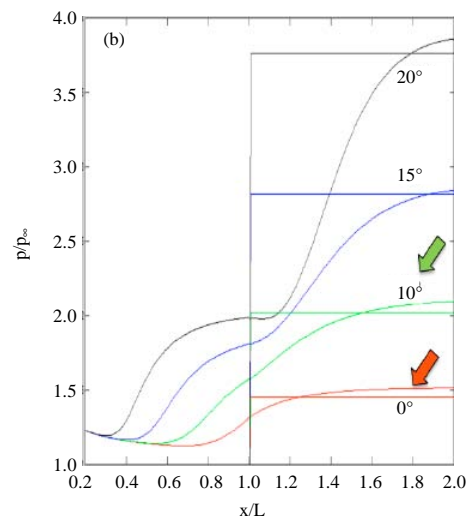


Fig. 14 (a-b): Comparison between results from Carter and MATLAB results



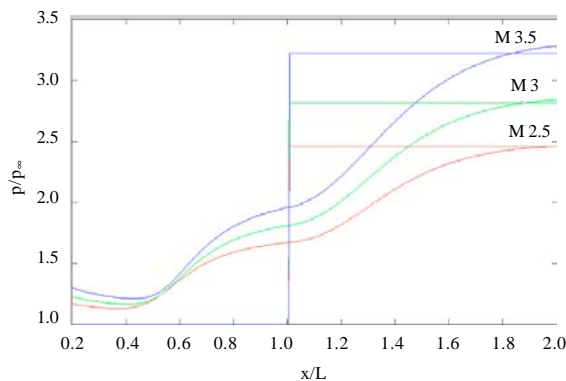


Fig. 15: Pressure profile for variable free stream velocity (Mach number)

### CONCLUSION

This research had investigated the supersonic flow over 2-dimensional compression corner for both inviscid and laminar case. Analysis were conducted for the cases of corner angle 5, 10 15 and 20 degree at free stream velocity of Mach 3 (variable angle), as well as the cases of free stream velocity Mach 2.5, Mach 3 and Mach 3.5 at corner angle 15 degree (variable free stream velocity). Numerical program had been developed using MATLAB and the results were validated through analytical solution, as well as results from results from previous researchers. Several conclusions can be drawn from the study:

- As the corner angle increases, the pressure imposed on the ramp increases for inviscid case. Meanwhile, for laminar case, the peak pressure increases, separation tends to occur and the recirculation region becomes more obvious
- As the free stream velocity (Mach number) increases, the pressure acting on the ramp increases for inviscid case. Meanwhile, for laminar case, the peak pressure increases while the recirculation region tends to diminish

For recommendation, other numerical schemes with higher accuracy such as Cubic Interpolation Profile (CIP), Total Variation Diminishing (TVD), Essentially Non-Oscillatory Scheme (ENO), etc., may be employed for future research in simulating the problem for results comparison. Besides, the problem can also be extended into the case of supersonic turbulent flow over compression corner to explore the difference between the laminar and turbulent case. Apart from obtaining the numerical results, it is suggested that experimental investigations can be carried out in order to develop a deeper understanding on this research.

### REFERENCES

- Anderson, J.D., 1995. Computational Fluid Dynamics: The Basics with Applications. McGraw-Hill, New York, USA.
- Brailovskaya, I., 1971. Flow in the near wake. Sov. Phys. Dokl., 16: 107-110.
- Carter, J.E., 1972. Numerical solutions of the Navier-Stokes equations for the supersonic laminar flow over a two-dimensional compression corner. NASA Technical Report No. R-385, pp: 1-84. [http://ntrs.nasa.gov/archive/nasa/casi.ntrs.nasa.gov/19720019661\\_1972019661.pdf](http://ntrs.nasa.gov/archive/nasa/casi.ntrs.nasa.gov/19720019661_1972019661.pdf)
- Cebeci, T., A.M.O. Smith and G. Mosinski, 1970. Calculations of compressible adiabatic turbulent boundary layers. Am. Instit. Aeronautics Astronautics J., 8: 1974-1982.
- Dogrusoz, S. and M.S. Kavsoglu, 2001. Numerical solution of hypersonic compression corner flows. Am. Instit. Aeronautics Astronautics J., 1750: 1-10.
- Dwyer, D.L., 1973. Supersonic and hypersonic two-dimensional laminar flow over a compression corner. Am. Instit. Aeronautics Astronautics J., 3007: 69-83.
- Holden, M.S. and J.R. Moselle, 1969. Theoretical and experimental studies of the shock wave-boundary layer interaction on compression surface in hypersonic flow. CALSPAN Report. No. AF-2410-A-1.
- Hung, C.M. and R.W. MacCormack, 1976. Numerical solutions of supersonic and hypersonic laminar flows over a two-dimensional compression corner. Am. Instit. Aeronautics Astronautics J., 14: 475-481.
- Kubota, T., L. Lees and J.E. Lewis, 1968. Experimental investigation of supersonic laminar, two-dimensional boundary-layer separation in a compression corner with and without cooling. Am. Instit. Aeronautics Astronautics J., 6: 7-14.
- Malinson, S.G., S.L. Gai and N.R. Mudford, 1992. Laminar flows of high enthalpy air in a compression corner. Proceedings of the 11th Australian Fluid Mechanics Conference, December 14-18, University of Tasmania, pp: 275-278.
- Werle, M.J. and S.D. Bertke, 1972. A finite-difference method for boundary layers with reverse flow. Am. Instit. Aeronautics Astronautics J., 10: 1250-1252.